Chapter 6.—Use of Airborne Near-Infrared LiDAR for Determining Channel Cross-Section Characteristics and Monitoring Aquatic Habitat in Pacific Northwest Rivers: A Preliminary Analysis

Russell N. Faux[1], John M. Buffington[2], M. German Whitley[1], Steve H. Lanigan[3], Brett B. Roper[4]

Abstract

Aquatic habitat monitoring is being conducted by numerous organizations in many parts of the Pacific Northwest to document physical and biological conditions of stream reaches as part of legal- and policy-mandated environmental assessments. Remote sensing using discrete-return, near-infrared, airborne LiDAR (Light Detection and Ranging) and high-resolution digital imagery may provide an alternative basis for measuring physical stream attributes that are traditionally recorded by field crews in these monitoring efforts. Here, we compare physical channel characteristics determined from airborne LiDAR versus those measured from field surveys using a total station. Study sites representing three different channel types (plane-bed, pool-riffle, and step-pool) with bankfull widths ranging from 2.5 to 18.6 m were examined in the upper John Day River basin, Oregon. LiDAR was flown on each study reach at a native pulse density of about 4 pulses/m^2, with up to four returns per pulse. Channel cross sections and stream gradient were determined from LiDAR-derived digital elevation models (DEMs) and directly compared to total station measurements. The ability to remotely sense bankfull elevations and associated channel geometry was of particular interest in this study. Because bankfull mapping from LiDAR depends on topographic indicators (breaks in streambank slope), bankfull elevation was determined objectively from plots of hydraulic depth (flow area divided by width) as a function of flow height at each cross section, with bankfull defined as the maximum value of this function, or as the first plateau in the hydraulic depth function in channels with multiple terraces. The latter definition allows a blind test of remote sensing capabilities for cases where no field observations of bankfull elevation are available.

Preliminary results show that, with the exception of one outlier, the first-terrace elevations determined from LiDAR DEMs differed from those of the total station by 0–40 cm (15 cm RMSE), corresponding channel widths differed by 0.23–5.23 m, and reach-average water-surface slopes differed by 0.0–0.0018 m/m. Furthermore, the LiDAR-derived cross-sectional profiles generally corresponded with those of the total station measurements above the water-surface elevation. However, first-terrace elevations frequently differed from field observations of bankfull stage, indicating that successful remote sensing of bankfull geometry using airborne LiDAR requires field observations to train identification of bankfull topography in LiDAR DEMs. When properly applied, remote sensing using airborne LiDAR has the potential to extend the spatial coverage, speed, consistency, and precision of physical stream measurements compared to existing field based techniques, and can be used to quantify higher-order topographic metrics (e.g., areas, volumes, curvature, and topology) beyond the point and line metrics currently measured by channel monitoring programs.

Introduction

Each year hundreds of personnel are fielded by monitoring programs to collect data on aquatic and riparian conditions of streams in the western United States. The organizations participating in these programs are tasked with determining the status and trend of aquatic ecosystems across large areas. For example, the Aquatic Riparian Effectiveness Monitoring Program (Reeves et al., 2004) is an interagency group organized to evaluate the success of the Northwest Forest Plan (U.S. Department of Agriculture, Forest Service; U.S. Department of Interior, Bureau of Land Management, 1994) and is responsible for monitoring aquatic and riparian

[1]Watershed Sciences, Inc., 257B SW Madison Ave, Corvallis, OR 97333

[2]U.S. Forest Service, Rocky Mountain Research Station, Idaho Water Center, 322 E. Front St., Boise, Idaho 83702

[3]U.S. Forest Service/Bureau of Land Management, Aquatic Riparian Effectiveness Monitoring Program, 333 SW First Ave., Portland, OR 97208

[4]U.S. Forest Service, Fish and Aquatic Ecology Unit, Utah State University, 860 N. 1200 E., Logan, Utah 84321

conditions across three States and 57 million acres (Reeves et al., 2004). Similarly, the PACFISH/INFISH Biological Opinion Program is focused on monitoring federal lands in the Upper Columbia River Basin, a region that covers subwatersheds in six States (Kershner et al., 2004). In many cases, these monitoring programs do not directly measure biological parameters, but infer habitat and ecosystem condition from physical surrogates. For example, channel characteristics (e.g., width, depth, residual pool depth) are used to assess availability and quality of habitat for aquatic organisms.

As one might expect, there are challenges associated with long-term monitoring over large areas, given typically limited resources. The number of sites sampled per year is relatively low, hindering spatial and temporal detection of differences in ecosystem condition and trends (Roper et al., 2002). In addition, while observer consistency and repeatability is critical for successful monitoring of watershed trends, recent studies show that observer variability in these monitoring efforts can be problematic (Whitacre et al., 2007; Roper et al., 2008; Roper et al., in prep). One potential solution to these problems is the use of remote sensing, as it can provide objective, repeatable measurements over broad spatial scales.

Airborne LiDAR (light detection and ranging) is a remote sensing technology that is currently being used to develop high-resolution topographic and vegetation models. Several recent studies show the potential for using LiDAR to map many of the physical parameters commonly quantified in aquatic and riparian monitoring efforts. For example, Jones (2006) used a LiDAR-derived digital elevation model (DEM) to map side channels and to identify potential sites for restoration of salmon habitat in the Dosewallips River, western Oregon. In other applications, James et al. (2007) documented the potential for using LiDAR to map headwater streams under canopy in Sumter National Forest, North Carolina, and Cavalli et al. (2007) used LiDAR to detect the spatial extent of different stream types in the Italian Alps.

Two LiDAR instruments provide a variety of applications for aquatic habitat monitoring: near-infrared and green-wavelength LiDAR. Near-infrared LiDAR can not penetrate water and is therefore used to map topography above the wetted channel. Green-wavelength devices can penetrate water to determine channel depth and provide seamless maps of both the aquatic and terrestrial environments (Wright et al., 2006; Kinzel et al., 2007; McKean et al., 2008). Although green-wavelength LiDAR can map many of the physical channel characteristics used in aquatic monitoring in a continuous and spatially extensive manner, near-infrared LiDAR instruments are currently capable of significantly higher pulse rates and, therefore, can map terrestrial environments at higher topographic resolutions. Although small-footprint green-wavelength LiDAR (Wright et al., 2006) has the potential to significantly change how aquatic monitoring is conducted, its commercial availability is limited and the widespread application of this technology is still several years in the future.

Near-infrared LiDAR data and derived products (topographic and vegetation models) are becoming increasingly available to resource managers in the Pacific Northwest. Several regional initiatives for the acquisition and distribution of high-resolution LiDAR data are underway in the Pacific Northwest (fig. 1). In Washington, the Puget Sound LiDAR Consortium (PSLC) has acquired 4.9 million acres of LiDAR coverage since 2001. In addition to specific projects led by agencies and private entities, the recently formed Oregon LiDAR Consortium (OLC) has initially contracted to acquire 1.3 million acres in western Oregon, with an additional 3.5 million acres anticipated over the next 3 years. These data are now available to resource managers and are now enhancing our ability to assess habitat condition over multiple spatial scales.

During the summer of 2005, the Pacific Northwest Monitoring Partnership (PNAMP) conducted a study in the John Day basin, northeastern Oregon, to examine the performance and compatibility of field protocols used by different aquatic habitat monitoring programs (Lanigan et al., 2006; Roper et al., in prep.). As part of this project, intensive total station surveys were conducted to better describe the channel characteristics of each study site (Roper et al., in prep.). Airborne near-infrared LiDAR and digital color imagery also were collected to analyze the ability of these data to characterize the physical habitat and riparian characteristics of the study sites. This paper focuses on the accuracy of channel characteristics determined from LiDAR-derived DEMs and, in particular, the ability to remotely sense bankfull elevations and associated channel geometry. Preliminary results are presented, comparing remotely sensed channel characteristics to those obtained from total station field surveys.

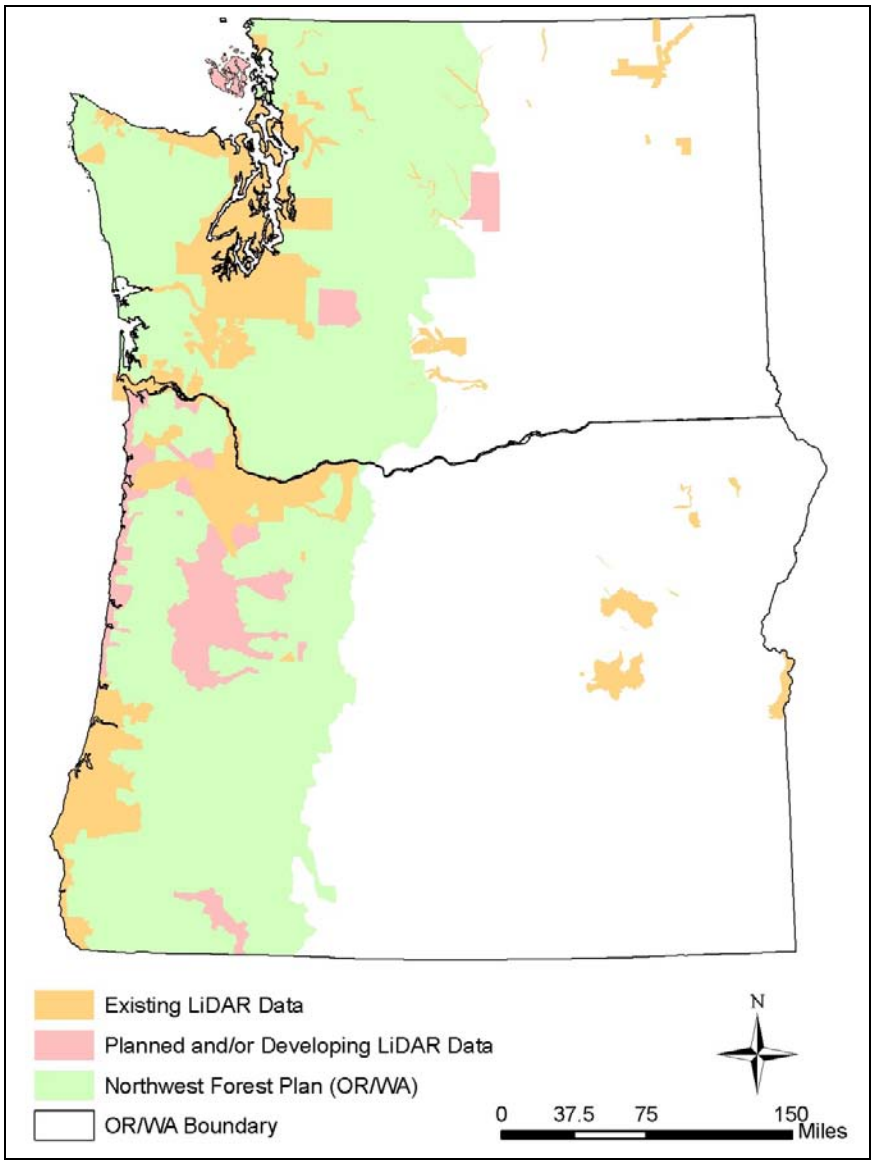

Figure 1. Monitoring region for the Aquatic and Riparian Effectiveness Monitoring Program (Reeves et al., 2004) in Oregon and Washington (part of the Northwest Forest Plan area) relative to spatial coverages of high-resolution LiDAR data that are either currently available or planned in 2009 for Oregon and Washington.

Study Area and Methods

Study Area

Eight mountain stream reaches were examined in the upper John Day River basin in northeastern Oregon (fig. 2). All streams were wadable, with bankfull widths ranging from 3.1 to 14.7 m, reach-average slopes from 0.94 to 9.7%, and median grain sizes (D_{50}) of 11.8–121.3 mm (table 1). The sampled reaches were 40 bankfull widths in length and selected to include three channel types (pool-riffle, plane-bed, and step-pool) (fig. 3).

Table 1. Channel characteristics determined from ground-based surveys

Stream	Stream type	Bed slope (%)	Bankfull width (m)	D_{50} (mm)
Crane	pool-riffle	0.94	8.01	11.8
Trail	pool-riffle	1.63	9.86	52.7
Bridge	plane-bed	1.03	8.12	37.4
Camas[1]	plane-bed	0.96	14.71	104.0
Tinker	plane-bed	2.86	3.14	33.7
Crawfish	step-pool	5.07	6.38	121.3
Myrtle	step-pool	9.70	3.96	27.7
Whiskey	step-pool	6.67	4.10	72.7

[1]Values based on limited sampling; 5 permanent cross sections only.

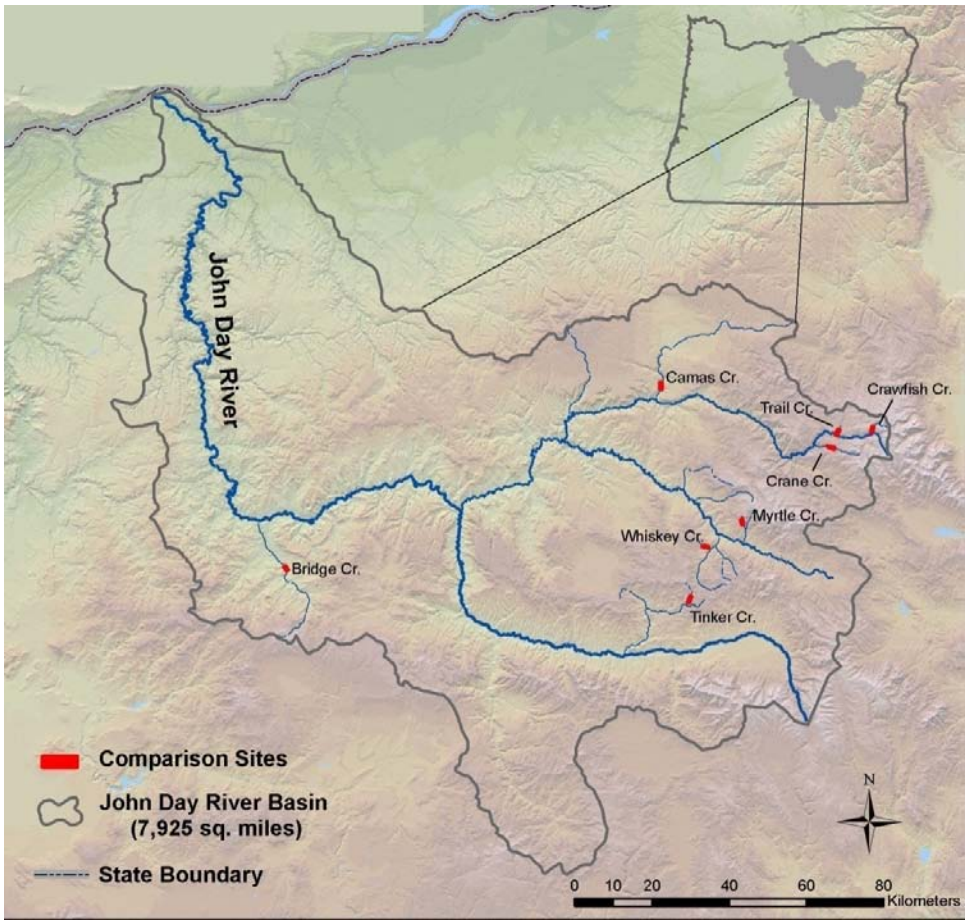

Figure 2. Study site locations within the John Day River basin, Oregon, USA.

Figure 3. Channel types examined in this study: (a) pool-riffle (Crane Cr.), (b) plane-bed (Camas Cr.) and (c) step-pool (Crawfish Cr.). See Montgomery and Buffington (1997) for further discussion of these channel types.

LiDAR Data

High-density LiDAR data were acquired for all eight sites from a fixed-wing platform, using an Optech 3100 ALTM system on September 28, 2005. The acquisition date was scheduled to correspond with late summer base-flow conditions in the study area, and early enough in the fall to avoid the possibility of early season snows that would interfere with LiDAR measurements. The settings consisted of a relatively narrow scan angle (±15°) and 50% overlap between opposing flight lines to increase laser pulse penetration through the canopy and to minimize shadowing by the vegetation (table 2). The vertical accuracy of the LiDAR data was assessed using 613 ground check points collected on hard, bare-earth surfaces (i.e., roads), and was found to have a root mean square error (RMSE) of 6.1 cm.

The raw LiDAR data were processed to produce geo-corrected coordinates for each laser return. Ground returns were classified from the raw point data using the TerraSolid processing software (TerraScan/TerraModeler from TerraSolid.fi) by implementing a series of filtering algorithms which defined the initial ground plane. The ground classification was then manually reviewed to remove any "clutter" or obvious misclassifications in the model. Across all sites, the average LiDAR pulse density was 3.1 pulses/m^2 with ground classified points having an average density of 1.2 returns/m^2 (table 2). The final ground-classified points were used to generate a 0.5 m DEM for each study reach, which took advantage of areas where the ground classified point density supported this resolution (fig. 4).

True color digital imagery was acquired coincidently with the LiDAR data using an Applanix Digital Sensor System 16 mega-pixel camera. The digital camera was integrated with a global positioning system (GPS) and inertial measurement unit, allowing direct geo-referencing of each pixel. The imagery was then orthorectified to the LiDAR DEM at a 15 cm (about 6 in.) ground sample distance, and was used to augment the interpretation of the LiDAR data.

Table 2. LiDAR system parameters.

System/acquisition parameter	Specification
Scan Angle	±15° from Nadir (30° total)
Number of Returns Collected Per Laser Pulse	4
Average Multi-Swath Pulse Density	3.1 pulses/m^2
Average Ground Return Density	1.2 returns/m^2
Adjacent Swath Overlap (Side-Lap)	≥ 50%
Assessed Vertical RMSE of LiDAR Survey	0.061 m

Total Station Data

Detailed topographic and geomorphic surveys of the study reaches were conducted from July 16 to September 12, 2005, using a Leica TPS1200 total station. Eighty cross sections were surveyed per reach, with cross sections placed at intervals of one-half the average bankfull width (fig. 5). Cross-sectional surveys recorded major topographic breaks, as well as water elevations, vegetation limits, bankfull elevations, floodplain topography, and hillslope margins in confined reaches. Because bankfull is defined as the elevation at which flow spills onto the floodplain (Leopold et al., 1964), it is relevant only to floodplain rivers. However, bankfull-equivalent indicators are commonly used in confined channels where floodplains are absent or poorly defined, as was the case for some of the plane-bed and step-pool channels examined in this study. Bankfull locations were identified based on the following standard field indicators (Dunne and Leopold, 1978; Harrelson et al., 1994), given in their order of reliance: break in bank slope corresponding with the active floodplain surface, high-flow markers (i.e., limit of bank scour, rock staining, sand/silt deposits, debris lines), vegetation limits, and bar tops. There is less confidence in perennial vegetation as a bankfull indicator because of its seasonal variability and interannual dependence on flow, scour and deposition. Similarly, bar tops typically indicate a lower-limit of bankfull flood stage because some additional depth of flow must occur over the tops of the bars for them to form through processes of sediment transport and deposition.

Five of the cross sections were monumented as reference sites for the PNAMP comparison of field monitoring protocols (Lanigan et al., 2006; Roper et al., in prep.). These cross sections were placed every 10 bankfull widths along the length of the channel and are referred to as "permanent cross sections" in this study (fig. 5).

The number of points sampled within the bankfull extent of each cross section ranged from 9 to 21 across the study sites, representing a point spacing of 5–13% of the bankfull width. In addition to cross sections, a longitudinal profile of the channel center-line was surveyed, as well as locations of all pool bottoms and downstream riffle crests. The overall data density within the bankfull channel typically was 0.4–3.7 points/m^2.

Although the survey points are accurate relative to each other, the coordinates for the benchmarks used in the total station surveys were recorded using a non-survey grade GPS and therefore the geographic precision of the benchmarks is unknown. The total station surveys were designed to compare to the other ground-based measurements being made as part of the comparison of monitoring protocols (Lanigan et al., 2006; Roper et al., in prep.), with the acquisition of airborne LiDAR data added late in the program. Therefore, precise geospatial references (i.e., surveyed benchmarks and/or air targets) were not included in the total station surveys.

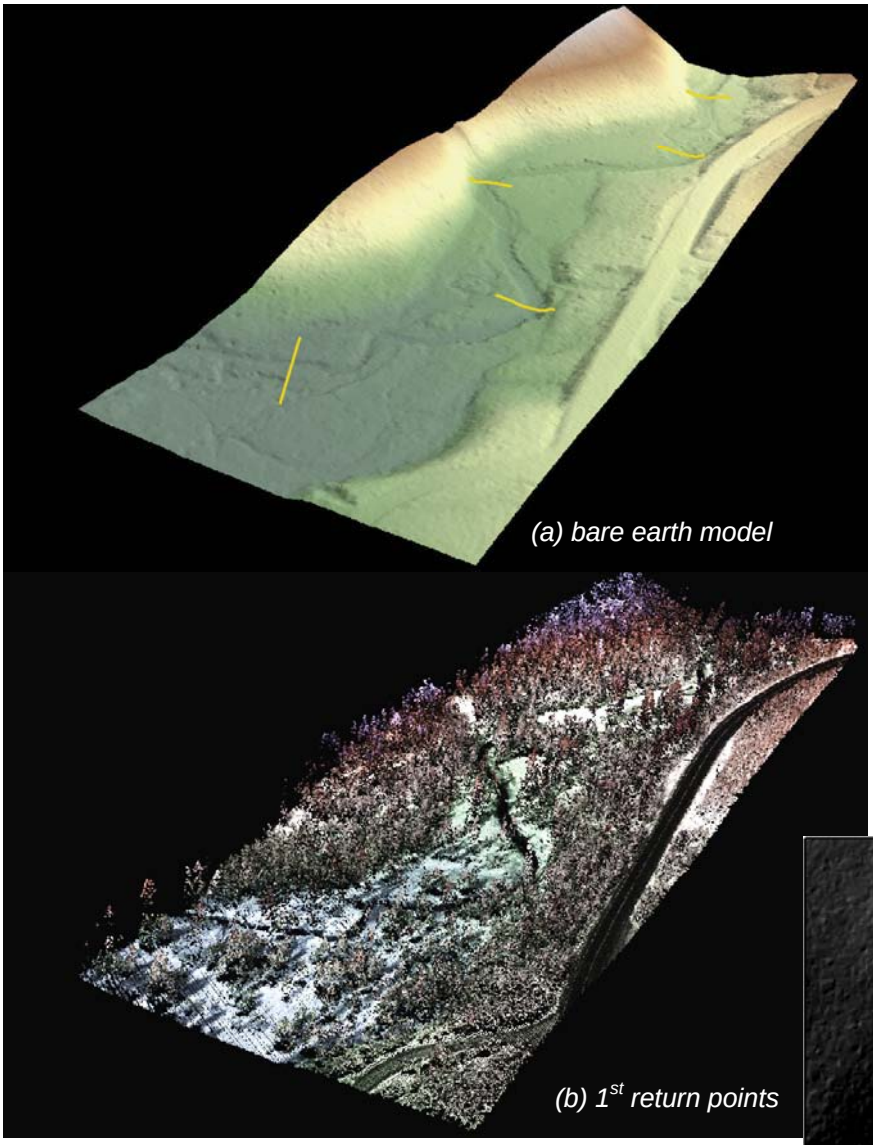

Figure 4. LiDAR-derived bare earth model (a) and LiDAR 1st return points (b) for Trail Creek. Yellow transects on the bare-earth model are the five monumented cross sections placed by the total station field crews.

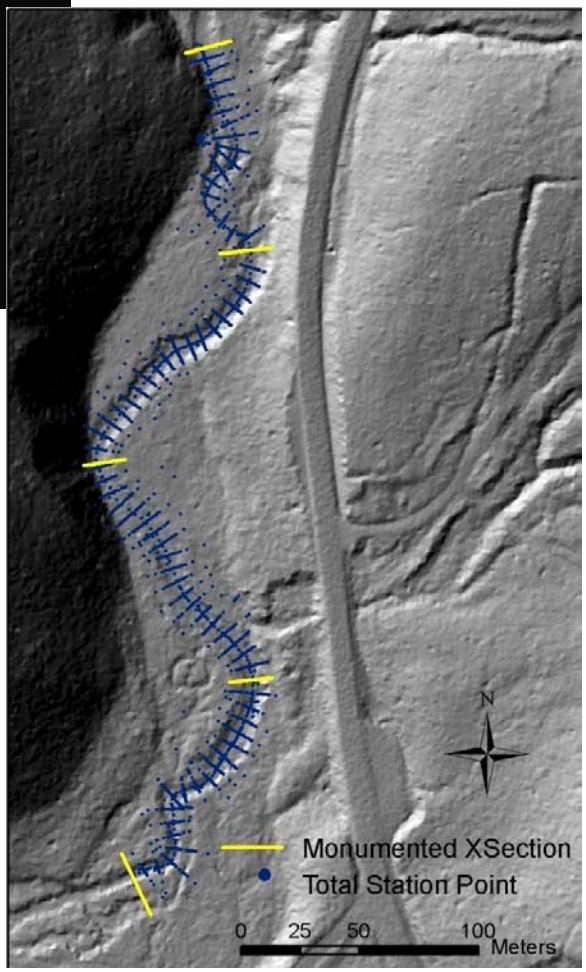

Figure 5. Locations of total station survey points ("ground points") and monumented cross sections on Trail Creek overlain on hillshade of the LiDAR 0.5-m DEM.

The lack of a good geographic reference was a potential source of error for comparing the geographically precise LiDAR points to the total station data.

For this analysis, we used a small subset of the available cross sections (two per site) for comparing channel characteristics determined from airborne LiDAR to those of the total station surveys. Our intent was to provide a preliminary comparison of the two approaches. Comparisons were conducted for monumented (or permanent) cross sections 2 and 4 (PXS2 and 4), located at longitudinal distances of 10 and 30 bankfull widths, respectively, in each study reach (fig. 5).

Analysis

Transect Placement

As a consequence of not having a precise geographic reference, some shifting in the horizontal (X, Y) plane was necessary to line-up the total station points with their true geographic coordinates. The X, Y shift was computed as a best-fit between the water-surface center line derived from the LiDAR DEM and the center-line profile measured by the total station crew. The five monumented cross sections in each reach were used as an additional reference, because hand-held GPS coordinates were available for the end-points of these cross sections. The shift maintained the integrity of the original data with no changes to the points relative to each other.

To accurately place the field data in the vertical dimension (Z), the relative elevations of the field measurements had to be given a true elevation datum. The water-surface elevation was used as a common datum for vertical alignment of the two data sets, and ortho-imagery was used to confirm the water-surface location in the LiDAR DEM. Although the datasets were collected at different times, both were collected during 2005 base-flow conditions, and differences in water-surface elevations between the two datasets were considered minimal (within a few cm) for these streams.

Channel Geometry

Once the total station transects were relocated relative to the LiDAR data, point elevations defining the channel cross sections were extracted along a corresponding transect in the LiDAR data. The ArcGIS extension EZ Profiler 9.1 (freeware) was used to generate the transect line and collect elevations from the LiDAR DEM at 0.5-m intervals.

The ability to remotely sense bankfull elevations and associated channel geometry is a key focus of this study. Bankfull elevation is a primary metric for fluvial studies (Leopold et al.. 1964) and commonly is used to scale and standardize channel characteristics relevant to aquatic habitat (e.g., Woodsmith and Buffington, 1996; Buffington et al., 2002). In the field, bankfull elevation is identified by a number of indicators, as discussed above (section, “Total Station Data”). In contrast, bankfull mapping from LiDAR depends almost entirely on topographic indictors (breaks in the streambank slope) identified from the LiDAR-derived DEM. In order to objectively compare bankfull elevations between the field- and LiDAR-based measurements, we plotted the hydraulic depth (flow area divided by width) as a function of flow height (elevation) at each cross section, where the maximum value of this function indicates a sudden increase in flow width at the elevation where water spills across the floodplain (i.e., bankfull) (fig. 6). This approach was suggested by McKean et al. (2005) and is a variant of the bankfull approaches discussed by Williams (1978).

We recognized that the above method for identifying bankfull elevation would work best in floodplain rivers and would be limited in confined channels that lack floodplains. The method is less definitive in channels with inset/multiple terraces, where one is faced with deciding which terrace and which plateau in the hydraulic depth function is the current bankfull elevation (i.e., the active floodplain) (fig. 7). Many of our study sites exhibited both characteristics confined channels and multiple terraces. Field observations can be used to guide selection of the correct overflow surface corresponding with the active floodplain (Williams, 1978), but we wished to conduct a blind test of the remote sensing capabilities of LiDAR (i.e., without recourse to field observations of bankfull). Consequently, where multiple terraces were present, we determined the elevation and channel width for the first terrace (i.e., lowest elevation terrace), which may or may not be equivalent to the actual bankfull elevation, depending on the local conditions and geomorphic history of a site. The hydraulic depth calculations were performed using the WinXSPRO program (Hardy et al., 2005) and were plotted versus elevation for the examined cross sections.

Stream Gradient

Water-surface elevations were measured from the LiDAR data by sampling directly from the DEM at 1-m intervals along the stream centerline. The stream centerline was generated using the flow accumulation function in ArcGIS Spatial Analyst and then manually edited within the GIS environment with the digital orthophotos as a visual reference. The extent of the study area was small enough that manual editing of the stream center was preferred for correcting for culverts and other features in the ground model that may create errors in the stream network. The custom ArcGIS extension TTools (Boyd and Kasper, 2005) was used to create equal-interval nodes along the centerline and to sample elevations directly from the DEM. LiDAR-derived water-surface slopes were compared to those determined from total station measurements at each site.

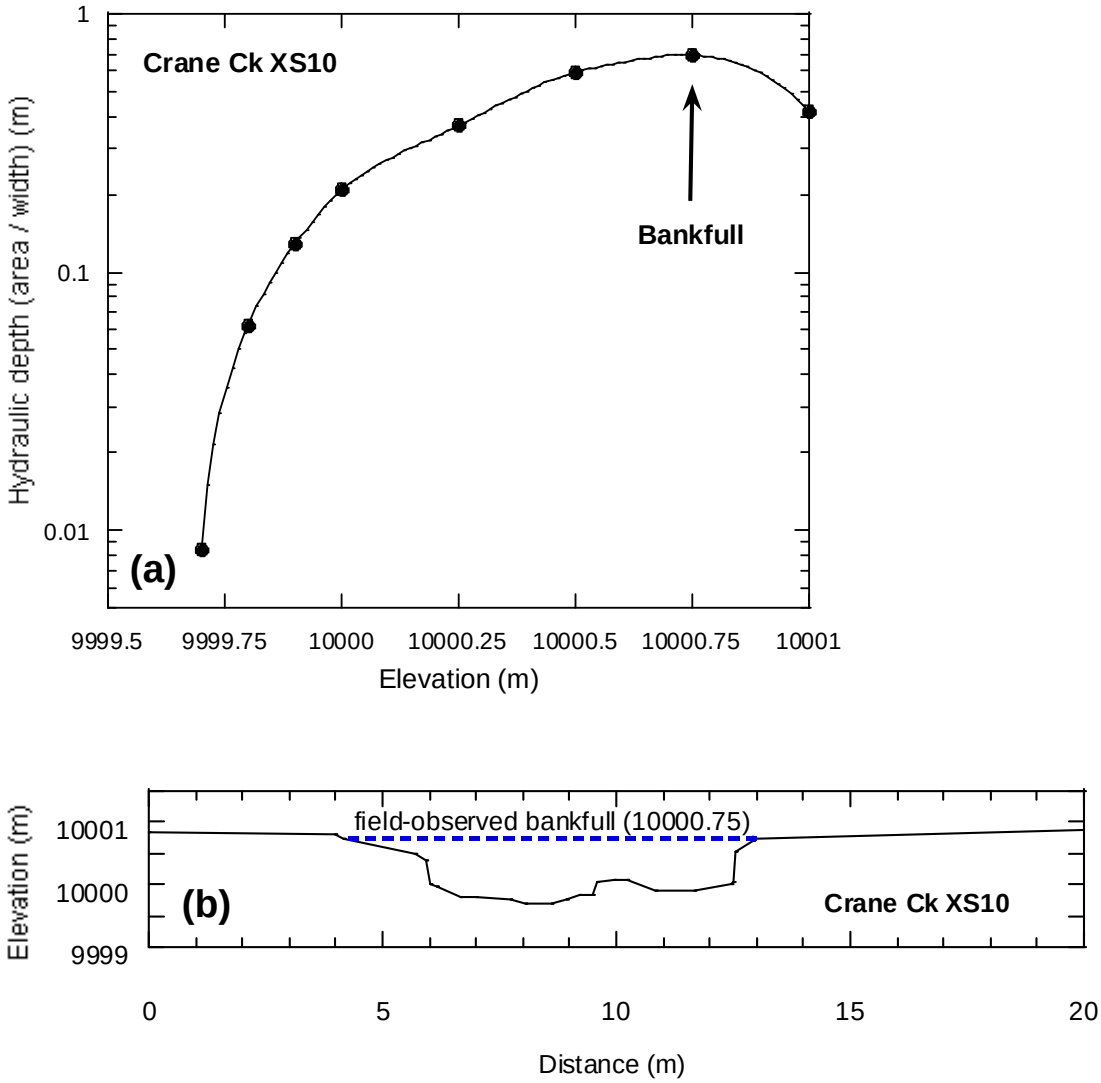

Figure 6. Example hydraulic depth function (a) for objectively defining bankfull elevation. The function maximum coincides with the active bankfull floodplain identified in the field (b, cross section). Reported elevations are for an arbitrary coordinate system and are not georeferenced.

Results

First Terrace Elevation and Bankfull Identification

With the exception of one outlier (Bridge Creek, PXS2), the first-terrace elevations derived from the LiDAR DEMs differed from those of the total station surveys by 0–40 cm (table 3), with a RMSE of 15 cm (complete dataset, including the above outlier, yields an RMSE of 34 cm). In some cases, the first terrace corresponded with the bankfull elevation identified in the field (fig. 8, Trail Creek), while in other cases, it underestimated the actual bankfull surface (fig. 8, Crane Creek; bankfull is the second terrace, while the first "terrace" is a bar top). Hence, while the first-terrace elevations are comparable between the LiDAR-derived data and the total station data, remote predictions of bankfull geometry may have errors and will likely require field observations to guide extraction of this feature from the LiDAR data.

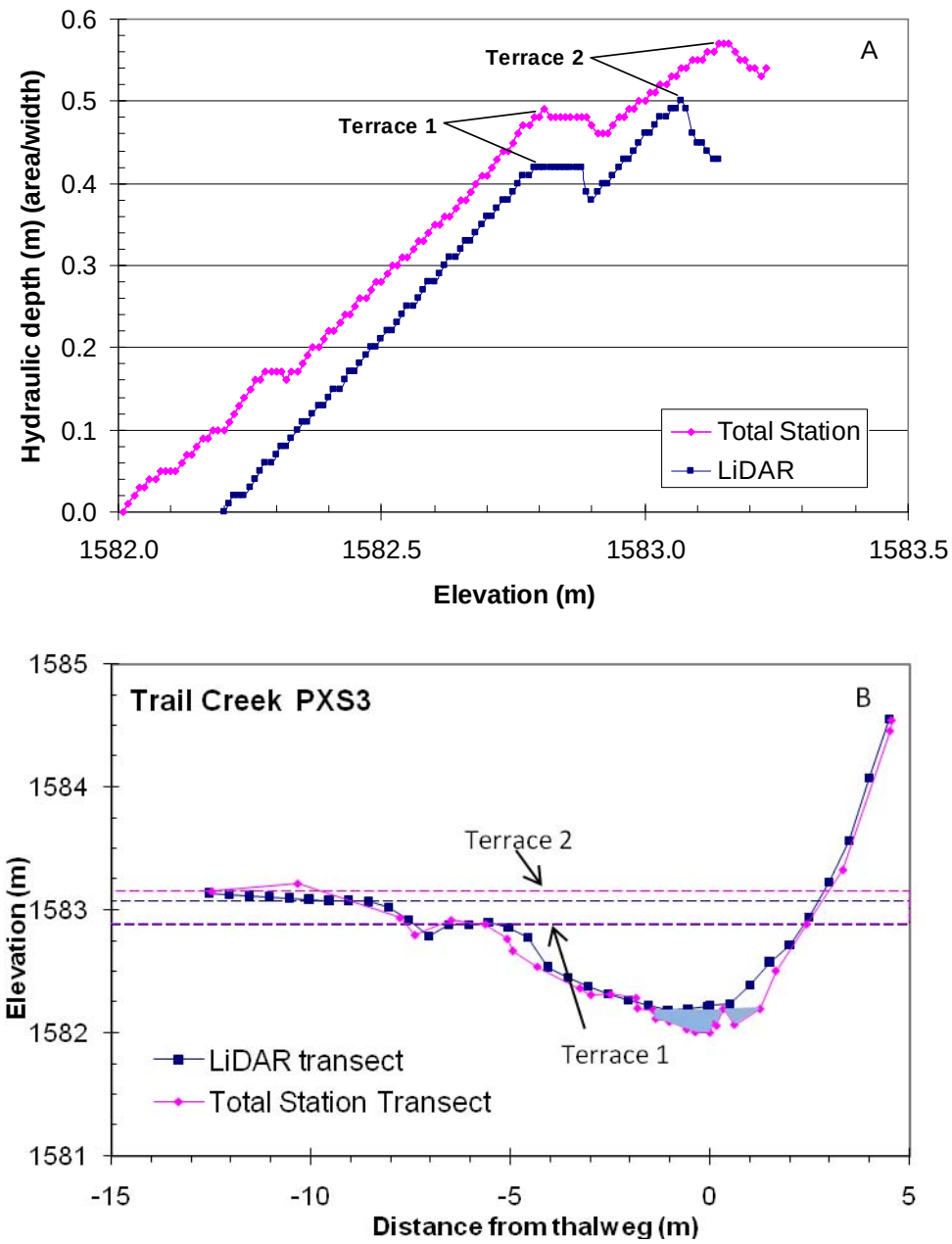

Figure 7. Example hydraulic depth function (a) and underlying cross section (b) for a channel showing two terraces. Dashed lines in (b) indicate terrace locations determined from (a).

Channel Widths

Comparisons between the LiDAR- and field-derived values of channel width at the first terrace of each cross section are shown in table 3. For plane-bed streams, a median difference of 0.87 m in channel width was observed between the two datasets. The LiDAR model overestimated channel width by 0.59–7.89 m (4–167 %) on four of the six measured cross sections, with an overall median error of 0.87 m (16%). The largest difference (7.89 m) was observed on Bridge Creek (PXS2) where the LiDAR-derived profile generalized the first terrace break and hence overestimated bankfull width. Excluding this cross section, the range of width overestimation decreases to 0.59–1.05 m (4–29%). At two of the six cross sections, the LiDAR model underestimated channel width by 0.35–2.34 m (8–13%).

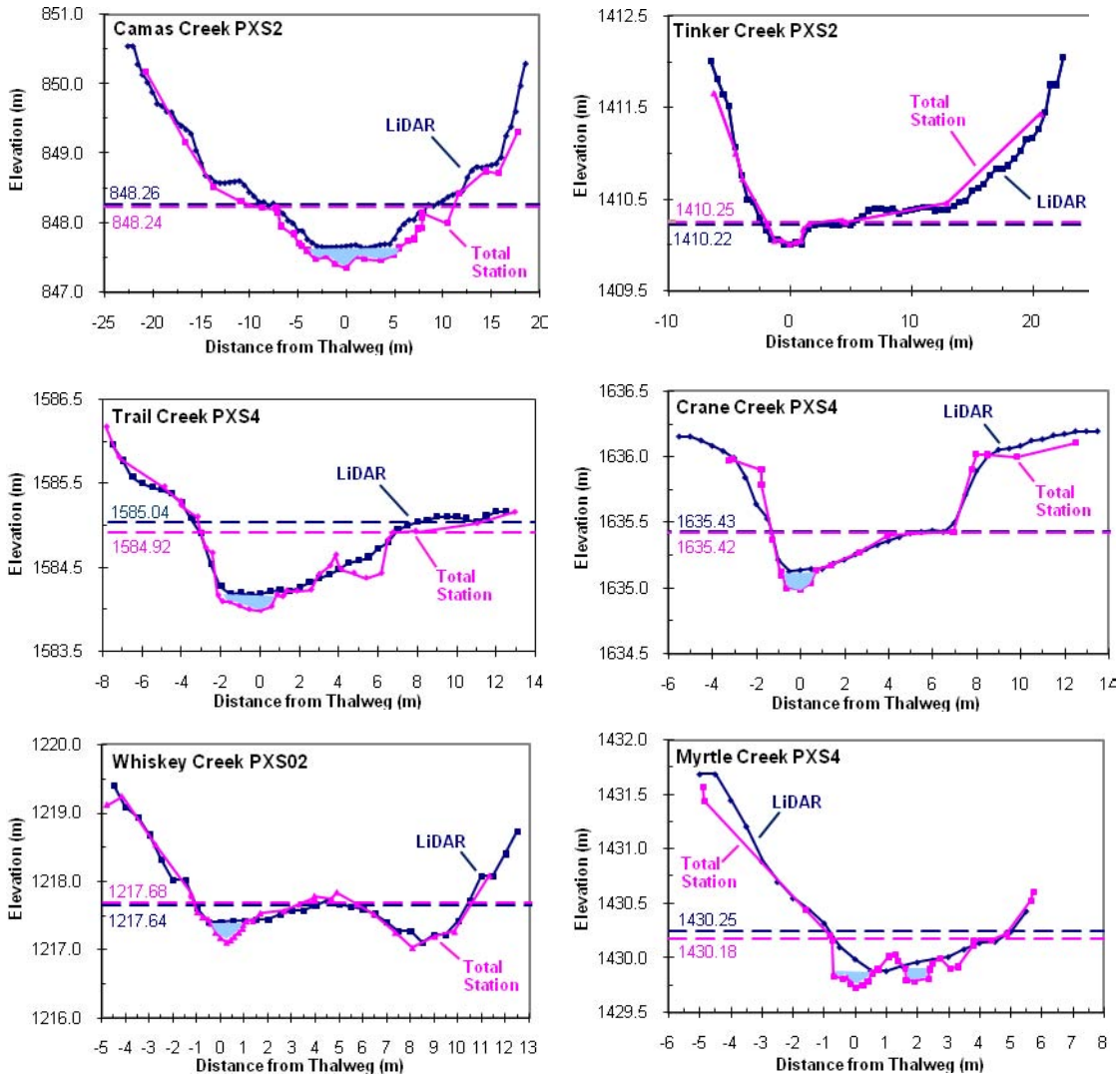

Figure 8. Comparison of LiDAR-derived and total station cross sections for plane-bed (top), pool-riffle (middle), and step-pool channels (bottom). Dashed lines are first-terrace elevations determined from the hydraulic depth method. The wetted channel is represented on the profile in blue and is based on field measurements. The water-surface topography is interpolated from the LiDAR DEM, which includes LiDAR returns from both the water surface and exposed channel topography.

For the pool-riffle streams, the comparison of LiDAR and field-derived values yielded a median difference in channel width of 1.57 m and a median error of 23%. The LiDAR model overestimated channel width by 0.40–1.89 m (4–76 %) for all four cross sections. Step-pool channels exhibited a median difference in channel width of 1.80 m and a median error of 43%. However, the frequency of over-versus under-estimation was equal in this channel type (3 overestimated and 3 underestimated).

These findings suggest that the accuracy of LiDAR-derived channel widths varies with channel type (progressively greater median errors across plane-bed, pool-riffle, and step-pool channels). The larger error in step-pool channels also may reflect limitations of the hydraulic depth approach for defining bankfull in confined streams. In several cases, plots of hydraulic depth versus elevation did not reveal a distinct local maximum. Consequently, a more robust approach or combination of methods should be considered for remote sensing of bankfull elevation across the range of stream types present in mountain rivers (e.g., Rosgen, 1994; Montgomery and Buffington, 1997).

Table 3. First-terrace elevations and widths determined from LiDAR versus total station data.

Stream	XSection	Terrence elevations (m)			Channel width (m)		
		LiDAR	Field	Difference	LiDAR	Field	Difference
Pool-Riffle Streams							
Trail	PXS2	1,581.31	1,581.31	0.00	9.91	9.51	0.40
Trail	PXS4	1,585.04	1,584.92	0.12	11.32	9.73	1.59
Crane	PXS2	1,634.31	1,634.21	0.10	4.39	2.50	1.89
Crane	PXS4	1,635.43	1,635.42	0.01	6.79	5.24	1.55
Plane-Bed Streams							
Camas	PXS2	848.24	848.26	-0.02	16.27	18.61	-2.34
Camas	PXS4	852.46	852.41	0.05	16.81	16.22	0.59
Tinker	PXS2	1,410.22	1,410.25	-0.03	4.18	3.49	0.69
Tinker	PXS4	1,412.19	1,412.24	-0.05	4.09	4.44	-0.35
Bridge	PXS2	660.17	658.94	1.23	12.63	4.74	7.89
Bridge	PXS4	660.19	660.01	0.18	4.68	3.63	1.05
Step-Pool Streams							
Whiskey	PXS2	1,217.64	1,217.68	-0.04	2.67	7.90	-5.23
Whiskey	PXS4	1,223.47	1,223.66	-0.19	3.45	5.57	-2.12
Myrtle	PXS2	1,423.62	1,423.37	0.25	4.62	2.90	1.72
Myrtle	PXS4	1,430.25	1,430.18	0.07	5.75	3.79	1.78
Crawfish	PXS2	1,797.46	1,797.06	0.40	7.24	5.43	1.81
Crawfish	PXS4	1,803.59	1,803.68	-0.09	5.47	5.70	-0.23

Channel Cross Sections

While the width predictions varied, the shape and topography of the cross-section profiles above the water-surface elevation were correlated between the two datasets, even for streams with channel widths of less than 5 m (fig. 8). In only one instance (Bridge Creek; PXS2) did the LiDAR DEM miss the first terrace, resulting in a significant overestimation of channel width (table 3). Inspection of the LiDAR DEM of Bridge Creek shows that the first terrace was visible as a continuous linear feature in the data and that the generalization of this terrace at PXS2 may have been the consequence of vegetation along the right bank rendering fewer ground returns. This finding suggests that sampling discrete cross sections in isolation from the spatially continuous dataset might be misleading.

We expected the LiDAR DEM to more precisely map the larger channel geometries due to a higher number of ground returns per cross section, with greater variability in results observed for smaller channel widths and fewer ground returns. Theoretically, the Nyquist frequency (twice the grid cell size) represents the minimum size of topographic features that can be delineated using a grid-based DEM (Warren et al., 2004; James et al., 2007). However, the LiDAR DEM described the channel geometry (in terms of terrace elevations and shape) of some of the smallest streams in the study (i.e., widths of 2–3 m). For example, the LiDAR DEM closely matched the field measured bank full elevation (within 3 cm) and width (within 70 cm) on Tinker Creek (PXS2), which had a field measured bankfull width of only 3.5 m. As expected, the DEM generally interpolated or missed features that were less than 1 m2 in planar surface area (i.e., less than 2× the DEM grid cell size; 0.5 m).

The accuracy of the LiDAR DEM depends on both the quality of the ground-point classification and the achieved ground return density. While the degree to which vegetation influences the LiDAR returns depends on season and species composition, heavily vegetated areas generally will result in fewer ground returns and the potential for more interpolation errors in the resulting DEM. This effect was evident in cases where the LiDAR DEM interpolated over fine-scale cross-sectional features and banks located under heavy vegetation. Landscape features such as downed logs also contributed to noise in the ground model. The largest inaccuracies were

observed when a combination of these factors contributed to the error budget. For example, permanent cross section 4 (PXS4) on Myrtle Creek contained both vegetation and downed logs near the streambank (fig. 9). Myrtle Creek also had one of the steepest gradients (table 1) and a confined channel. The DEM at this location generalized the steep terrace break along the left bank and completely missed the small channel split in the center of the stream, which appeared due to a mixture of relatively small channel width (<4 m) and downed logs/vegetation in the stream (fig. 9).

Stream Gradient

Stream gradients determined from the two data sets are in close agreement (table 4), with median errors of 3.87, 5.75, and 0.16 percent for pool-riffle, plane-bed, and step-pool channels, respectively. The difference in slope measurements between the two approaches generally decreases with channel gradient, with step-pool channels showing the least error (fig. 10).

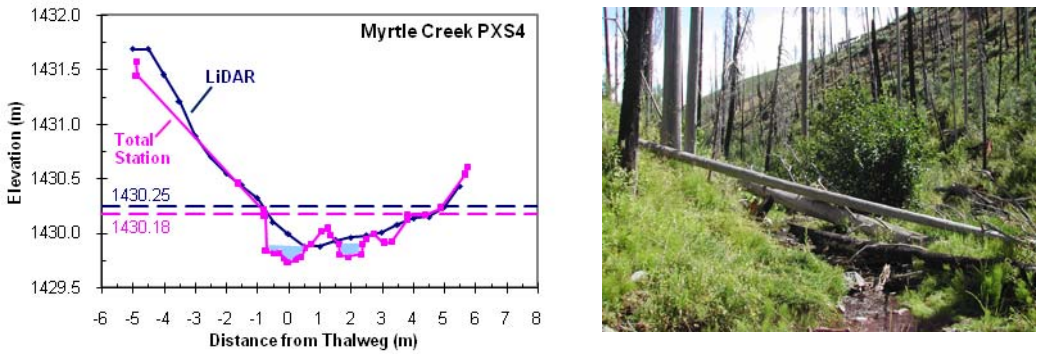

Figure 9. Example of fine-scale topography obscured by large woody debris and riparian vegetation in a LiDAR-derived cross section compared to that surveyed in the field with a total station. The ground-level photograph shows general channel conditions in Myrtle Creek.

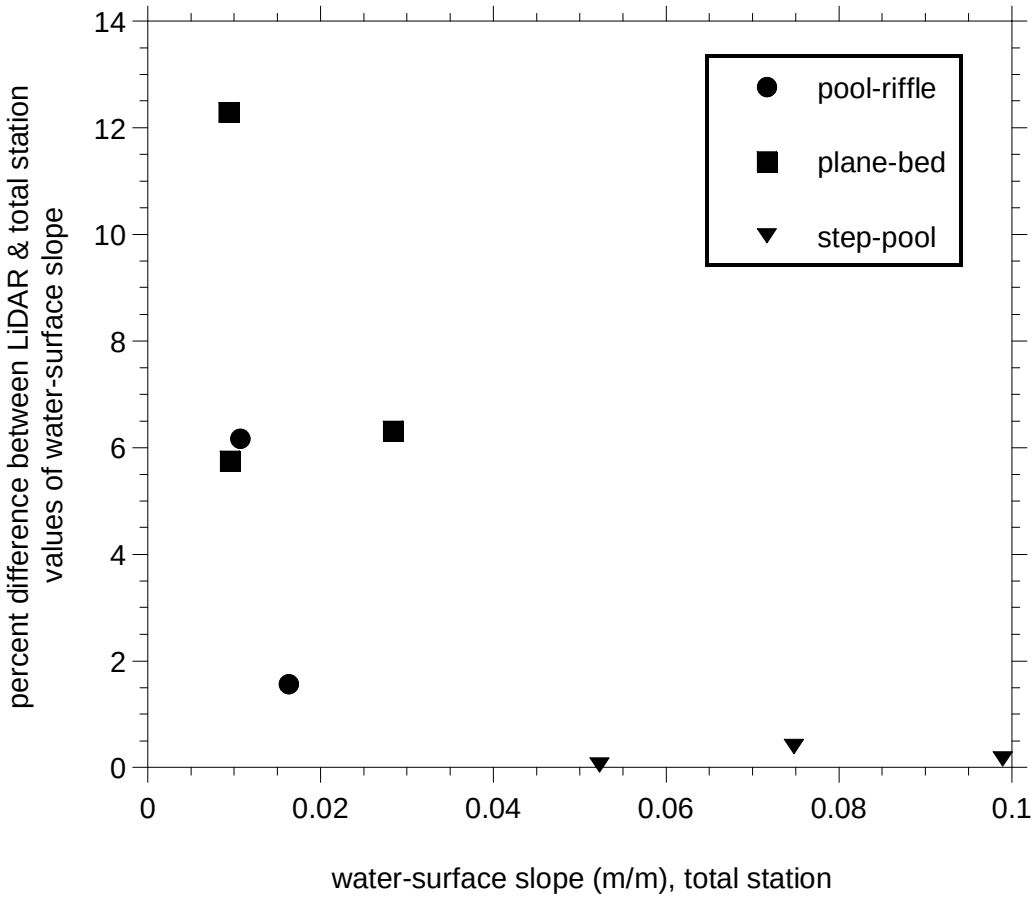

Figure 10. Scatter plot of percent difference in water-surface slope between LiDAR and total station measurements for different stream types.

While the gradient comparisons were based on a limited number of water surface measurements in the total station data, water surface elevations can be sampled from LiDAR data at any user defined interval (fig. 11). Dense sampling of the water-surface topography potentially can be used to locate pools and riffles (low-gradient, smooth surface areas relative to that of steeper-gradient, rough surface areas indicative of riffles and steps).

Table 4. Comparison of reach-average water-surface gradient between the total station data and the LiDAR DEM.

	Water-surface gradient (m/m)		
	LiDAR	Total station	Percent difference
Pool-Riffle Streams			
Trail Creek	0.0160	0.0163	1.56
Crane Creek	0.0101	0.0107	6.17
Plane-Bed Streams			
Camas Creek	0.0089	0.0095	5.75
Tinker Creek	0.0266	0.0284	6.32
Bridge Creek	0.0105	0.0094	-12.29
Step-Pool Streams			
Whiskey Creek	0.0745	0.0748	0.40
Myrtle Creek	0.0988	0.0990	0.16
Crawfish Creek	0.0523	0.0523	0.05

Discussion

Overall, the LiDAR approach tended to overestimate channel widths (69% of the time), with errors systematically varying with channel type (progressively greater median error across plane-bed, pool-riffle, and step-pool channels). Overestimation of channel width likely is due to the resolution of the LiDAR DEM and interpolation of streambank topography in locations where the density of ground returns is reduced by riparian vegetation. Some error also may be due to the native resolution of the data (section, “LiDAR Data Quality”). The geo-positioning of the field data could not be quantified, but inevitably introduced additional uncertainty due to small differences in the position or angle of the cross section.

Results also showed that remote sensing of the bankfull elevation and width using LiDAR may be prone to errors in channels with multiple terraces. However, these errors could be reduced with limited field observations that allow data training for selection of the terrace corresponding with the active floodplain.

While differences in width were observed between LiDAR-derived cross sections and those measured in the field, LiDAR offers a means to apply a consistent sampling method to all sites in a watershed and to reduce or eliminate observer variability in field sampling sites. Among observers, estimated bankfull dimensions have been shown to vary by as much as ±15 % (Roper et al., 2002). Furthermore, because the LiDAR data are geographically precise, temporal changes in channel geometry can be evaluated at the same location using the same

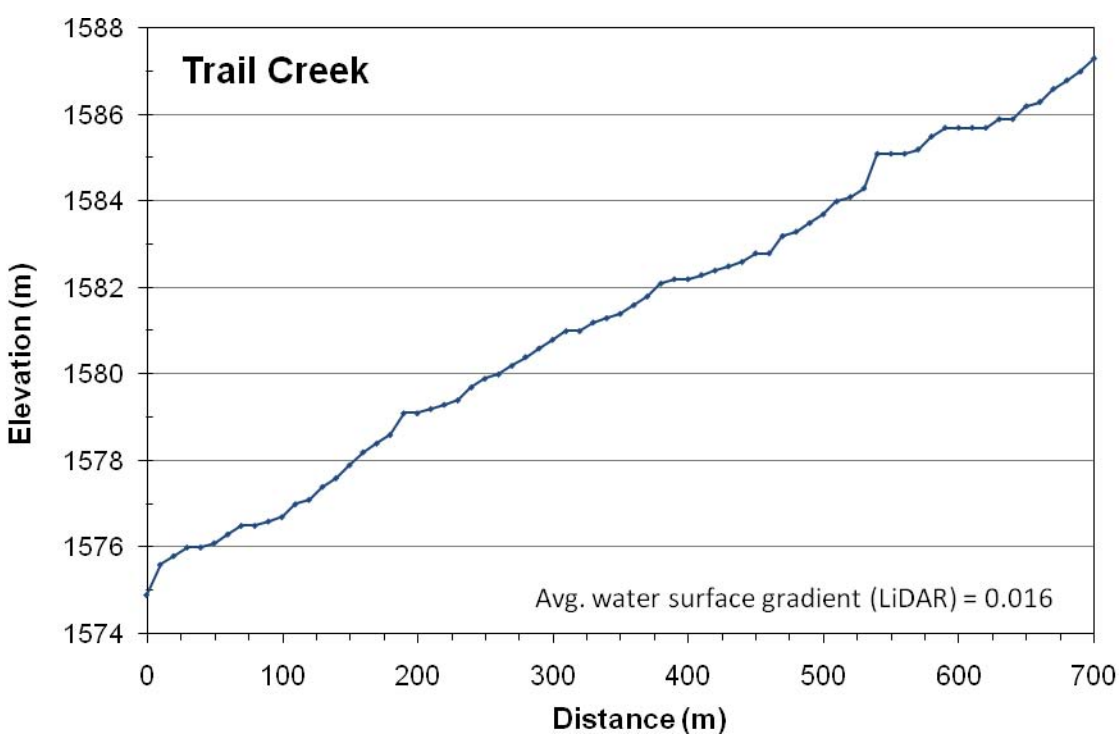

Figure 11. Example of water-surface elevations sampled from the LiDAR DEM at 1-m intervals longitudinally along Trail Creek (a pool-riffle stream).

methods. LiDAR-derived models have continued to improve through technological advances in pulse densities, GPS accuracy, and ground classification methods. Consequently, multi-temporal analysis should consider the contribution of differences in the precision and resolution of the underlying data when interpreting results.

Field crews typically measure channel cross sections at discrete locations along the channel. Although these survey points are accurate, even the most rigorous surveys are inherently limited due to time and resource constraints. Consequently, field measurements typically quantify physical habitat indicators at discrete locations, but often fail to accurately capture the variability of these parameters at the watershed or even reach scale. For example, Young et al. (2006) showed that quantifying the variability of large wood debris may require sampling over much longer stream lengths than typically measured during monitoring surveys. In contrast, LiDAR DEMs are spatially continuous and can be used to measure a variety of channel characteristics at user defined intervals along the stream, better quantifying the spatial variability of conditions. For example, first-terrace widths varied from 3.3–23.4 m over a 3-km segment of Trail Creek, showing a greater range of variability than would have been detected by the five monumented cross sections at this site (fig. 12). LiDAR mapping of these physical parameters provides an unprecedented ability to quantify channel characteristics and associated habitat at multiple spatial scales (e.g., McKean et al., 2008).

LiDAR Data Quality

The quality of results obtained from LiDAR will be strongly controlled by the native resolution and accuracy of the LiDAR data and derived products (table 2). A lower resolution data acquisition (expressed as pulse densities for raw LiDAR) may produce different results in terms of how well the DEM represents the channel geometry. James et al. (2007) showed that LiDAR data processed at 2-m grid cells were not suitable for detailed morphologic analysis or for subtle change detection in monitoring gullies in headwater streams in South Carolina. The number of ground returns can be improved by collecting data at higher pulse densities and flight planning that maximizes penetration through the canopy. In the Pacific Northwest, the Oregon LiDAR Consortium (OLC) and Puget Sound LiDAR Consortium (PSLC) are currently collecting data at pulse densities of >8 pulses/m^2 (PSLC has collected data at ≥4 pulses/m^2 since 2005). The collection of data during winter months also helps minimize the influence of broad-leaf riparian vegetation on ground return density. Finally, the LiDAR instrument has to be well calibrated with good relative consistency.

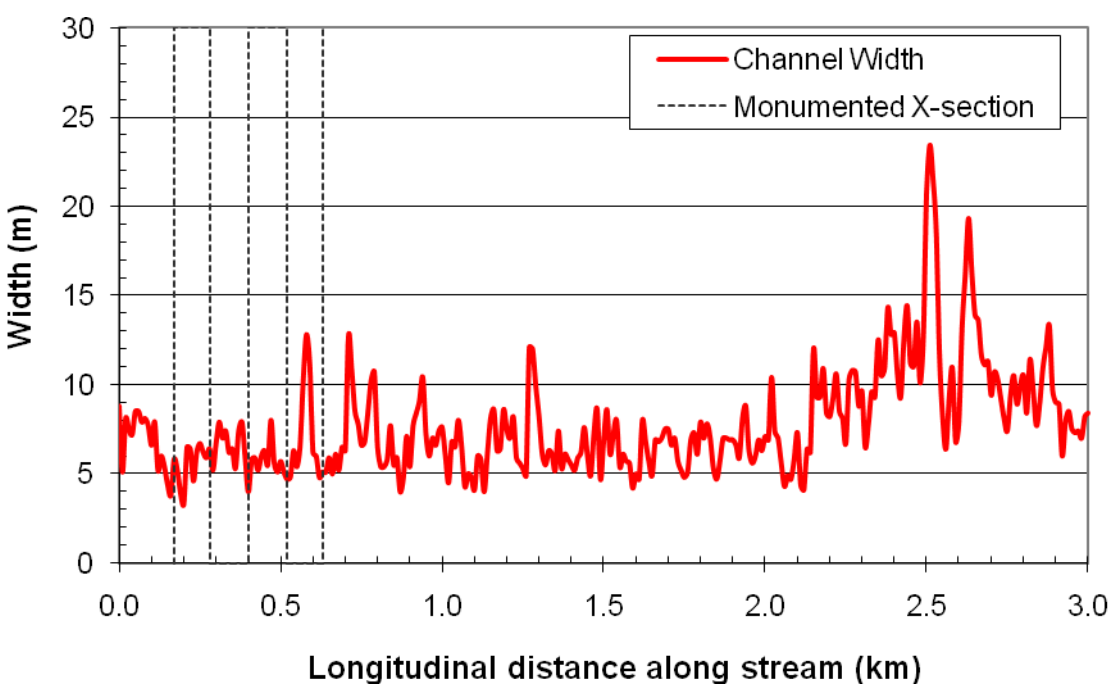

Figure 12. Plot showing first-terrace widths measured at 5-m intervals over three km of Trail Creek derived from the LiDAR data. The locations of the five monumented cross sections (fig. 5) also are shown on the plot.

Costs and Capabilities

With the increasing availability of high-resolution, quality-controlled LiDAR data through statewide initiatives and regional consortiums, natural resource managers can benefit by utilizing publicly available data and/or contributing to regional consortiums to collect data from new areas of interest. Large initiatives offer a pre-defined price structure that realizes an economy of scale by combining contributions from multiple entities. Current pricing through the Oregon and Puget Sound LiDAR Consortiums is $0.78/acre for contiguous areas greater than 250 mi^2 (Puget Sound LiDAR Consortium, 2008).

Although there are many potential benefits of using LiDAR (e.g, increased spatial sampling, elimination of observer variability), LiDAR measurements provide a subset of the attributes currently collected by aquatic habitat monitoring programs (table 5). Other attributes can be partially measured or inferred depending on scale and the availability of corresponding imagery. As technology continues to advance (e.g., increased pulse densities, small footprint green-wavelength LiDAR, etc.), the number of attributes that can be reliably measured also will advance. Currently, the benefit of LiDAR data products will be to enhance, but not replace, field monitoring programs.

Table 5. Near-infrared LiDAR capabilities for measuring channel and habitat attributes.

[**Measurable**: Y, parameter measurable with minimal error; WL, parameter measurable to some degree, with limitations under some circumstances; N, parameter can not be measured]

Parameter	Measurable	Comments
Channel characteristics		
- Reach length	Y	
- Sinuosity	Y	
- Connectivity	Y	Includes mapping inactive/paleo-channels
- Terrace Elevations	Y	
- Bank Incision	Y	Bank elevation/channel elevation
- Cross Sections	WL	Measured down to water surface
- Bankfull Depth	WL	Provides a reasonable estimate on small streams at base flow.
- Bank Angle	WL	Scale and ground-return density may be a factor on small streams in terms of how well bank topography can be identified.
- Bank Type	WL	
- Bank Stability	WL	
- Partial blockages to salmon migration	WL	Improved with digital imagery, but features that represent a real blockage may be open to interpretation.
- Water Surface Elevation	Y	
- Pool Frequency/Length	WL	Water-surface topography can be used to locate pools (low-gradient, smooth surface areas relative to that of steeper-gradient, rough surface areas indicative of riffles and steps). This capability will be a function of stream size and discharge (smoothness of water-surface profile), and can be facilitated with multi-spectral images.
- Pool Depth	N	
- Bed Topography	N	
- Substrate	N	
- Bank Materials	N	
Valley/Upslope		
- Valley cross section	Y	
- Landslides	Y	
- Road Density	Y	
- Stream Crossings	Y	
- Impervious Surfaces	Y	Improved with digital imagery.
Riparian		
- Vegetation Height	Y	
- Large Woody Debris	WL	The availability of large wood can be derived from LiDAR-derived vegetation models, but can be greatly improved with digital imagery.
Biological		
- Water Chemistry	N	
- Biology (fish, invertebrates, etc.)	N	

Conclusions

High-resolution LiDAR data and derived DEMs present an opportunity for resource managers to expand the amount and quality of information available for aquatic habitat monitoring. This paper specifically looked at the ability of LiDAR to describe the geometry and slope of mountain channels in northeastern Oregon. The LiDAR data offers the means to apply a consistent and repeatable approach for sampling and analysis of physical characteristics within the watershed. The elimination of errors introduced by observer interpretation will improve a manager's ability to compare results between streams and/or between years on the same stream.

Ultimately, the broader utility of LiDAR data is in the ability to develop higher-order topographic metrics (e.g., area, volumes, curvature, and topology) of homogeneous units rather than measuring point or line samples common to existing protocols. Because near-infrared LiDAR does not penetrate the water surface, the DEM does not contain information about the channel depth, bed topography, and substrate size. As a result, near-infrared LiDAR data are more useful for understanding riparian, floodplain, and upslope characteristics. The need for in-channel data for habitat monitoring and modeling fluvial processes warrants continued technological development and deployment of high-resolution bathymetric (green wavelength) LiDAR. In both cases, the increased availability of these data will allow field crews to focus more time on studying the biological processes occurring within the wetted channel and to sample over larger spatial areas for the remaining parameters that can not be determined remotely with LiDAR.

LiDAR-derived DEMs additionally provide the potential for extending decision support processes to include spatially explicit information that is not well represented in existing protocols. For example, stream slope, sinuosity, channel complexity, and LWD retention could be mapped continuously along the stream length, capturing the overall variability in the system (fig. 13). Although not explicitly addressed in this study, the LiDAR data inherently contain information on upslope factors that influence habitat quality, such as road location, landslides, and riparian vegetation. In short, the availability of high-resolution LiDAR data may move our view of physical habitat monitoring away from discrete subsamples to a watershed-scale view that captures more of the complexity and variability of the ecosystem condition.

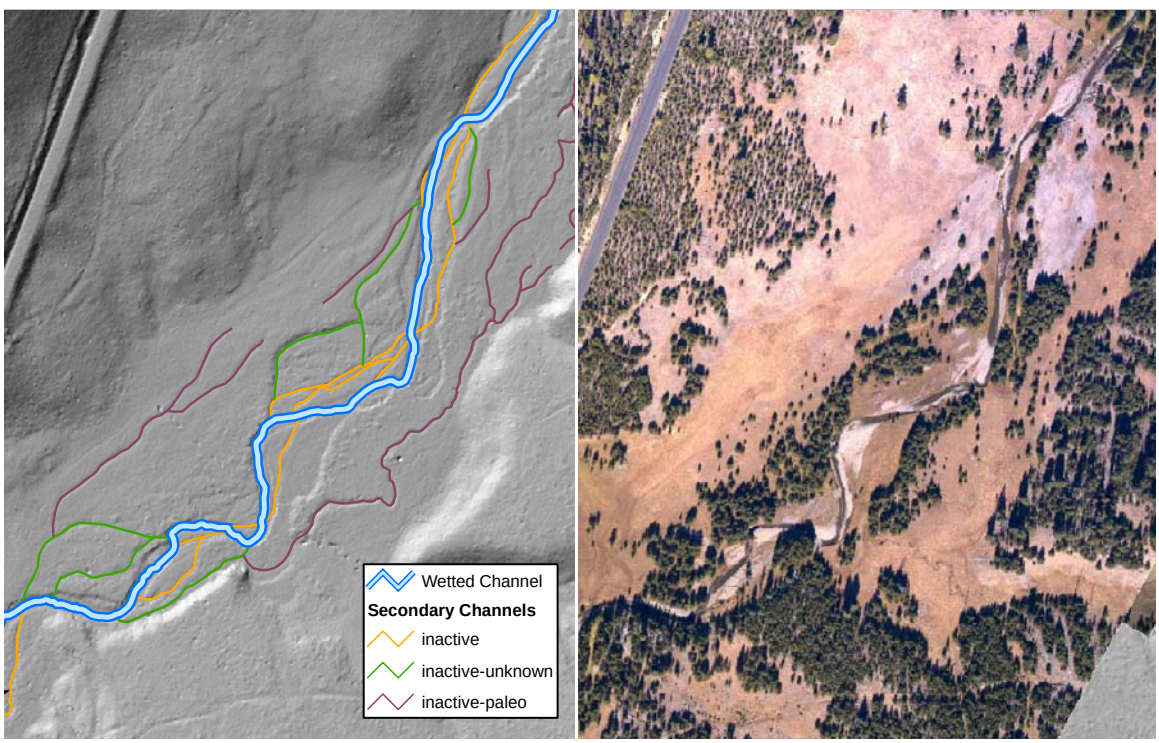

Figure 13. Example showing the mapping of side and secondary channels along a section of Trail Creek. Mapping of side-channel and floodplain elevations can provide measures of aquatic and riparian habitat suitability that extend beyond traditional monitoring parameters.

Acknowledgments

Funding for the LiDAR data acquisition and analysis was provided by NOAA Fisheries, Conservation Biology Division, Montlake Blvd East, Seattle, WA. We thank Rick Champion, Tom Frost, Jim McKean, and Keith Wolf for comments that improved the manuscript. Special thanks also to the Pacific Northwest Aquatic Monitoring Partnership for their support of this project.

References

Boyd, M., and Kasper, B., 2005, TTools program for ArcView: Oregon Department of Environmental Quality, accessed June 2008, http://www.deq.state.or.us/wq/tmdls/tools.htm

Buffington, J.M., Lisle, T.E., Woodsmith, R.D., and Hilton, S., 2002, Controls on the size and occurrence of pools in coarse-grained forest rivers: River Research and Applications, v. 18, no. 6, p. 507-531.

Cavalli, M., Tarolli, P., Marchi, L., and Fontana, G.D., 2007, The effectiveness of airborne LiDAR data in the recognition of channel bed morphology: Catena, v. 73, p. 249-260.

Dunne, T., and Leopold, L.B., 1978, Water in Environmental Planning: Freeman, San Francisco, California, 522 p.

Hardy, T., Panja, P., and Mathias, D., 2005, WinXSPRO, A channel cross section analyzer, User's Manual, Version 3.0: USDA Forest Service General Technical Report RMRS-GTR-147, Rocky Mountain Research Station, Fort Collins, CO, 94 p.

Harrelson, C.C., Rawlins, C.L., and Potyondy, J.P., 1994, Stream channel reference sites: An illustrated guide to field technique: U.S. Department of Agriculture, Forest Service, Rocky Mountain Forest and Range Experiment Station General Technical Report GTR-RM-245, 61 p.

James, L.A, Watson, D.G., and Hansen, W.F., 2007, Using LiDAR data to map gullies and headwater streams under forest canopy: South Carolina, USA, Catena, v. 71, p. 132-144.

Jones, J., 2006, Side channel mapping and fish habitat suitability analysis using LiDAR topography and orthophotography: Photogrammetric Engineering and Remote Sensing, v. 72, no. 11, p. 1202-1206.

Kershner, J.L., Archer, E.K., Coles-Ritchie, M., Cowley, E.R., Henderson, R.C., Kratz, K., Quimby, C.M., Turner, D.L., Ulmer, L.C., and Vinson, M.R., 2004, Guide to effective monitoring of aquatic and riparian resources: USDA Forest Service General Technical Report RMRS-GTR-121, Rocky Mountain Research Station, Fort Collins, CO, 57 p.

Kinzel, P.J., Wright, C.W., Nelson, J.M., and Burman, A.R., 2007, Evaluation of an experimental LiDAR for surveying a shallow, braided, sand-bedded river: Journal of Hydraulic Engineering, v. 133, no. 7, p. 838-842.

Lanigan, S., Roper, B., Buffington, J.M., Archer, E., Downie, S., Faustini, J., Hubler, S., Jones, K., Merritt, G., Konnoff, D., Pleus, A., Ward, M., and Wolf, K., 2006, Pacific Northwest side-by-side protocol comparison test: 5th National Water Quality Monitoring Conference, Monitoring Networks: Connecting for Clean Water, San Jose, CA.

Leopold, L.B., Wolman, M.G., and Miller, J.P., 1964, Fluvial processes in geomorphology: Freeman, San Francisco, CA, 522 p.

McKean J.A., Isask, D.J., and Wright, C.W., 2005, Mapping channel morphology and stream habitat with a full wave-form green lidar: EOS Transactions, American Geophysical Union, v. 86, no. 52, Fall Meeting, Suppl. Abstract H34B-05.

McKean J.A., Isaak, D.J., and Wright, C.W., 2008, Geomorphic controls on salmon nesting patterns described by a new, narrow-beam terrestrial–aquatic lidar: Frontiers in Ecology and the Environment, v. 6, no. 3, p. 125-130.

Montgomery, D.R., and Buffington, J.M., 1997, Channel-reach morphology in mountain drainage basins: Geological Society of America Bulletin 109, p. 596-611.

Puget Sound LiDAR Consortium (PSLC), 2008, PSLC Documents: accessed June 2008, at http://pugetsoundlidar.ess.washington.edu/About_PSLC.htm

Reeves, G.H., Hohler, D.B., Larsen, D.P., Busch, D.P., Kratz, K., Reynolds, K., Stein, K.F., Atzet, T., Hays, P., and Tehan, M., 2004, Effectiveness monitoring for the aquatic and riparian component of the Northwest Forest Plan: conceptual framework and options: USDA Forest Service General Technical Report PNW-GTR-577, Pacific Northwest Research Station, Portland, OR, 71 p.

Roper, B.B., Kershner, J.L., Archer, E., Henderson, R., and Bouwes, N., 2002, An evaluation of physical habitat used to monitor streams: Journal of the American Water Resources Association, v. 38, p. 1637-1646.

Roper, B.B., Buffington, J.M., Archer, E., Moyer, C., and Ward, M., 2008, The role of observer variation in determining Rosgen stream types in northeastern Oregon mountain streams: Journal of the American Water Resources Association, v. 44, no. 2, p. 417-427.

Roper, B.B., Buffington, J.M., Bennett, S., Lanigan, S.H., Archer, E., Downie, S., Faustini, J., Hillman, T.W., Hubler, S., Jones, K., Jordan, C., Kaufmann, P.R., Merritt, G., Moyer, C., and Pleus, A., (in prep.), A comparison of the performance and compatibility of protocols used by seven monitoring groups to measure stream habitat in the Pacific Northwest.

Rosgen, D.L., 1994, A Classification of Natural Rivers: Catena, v. 22, p. 169-199.

U.S. Department of Agriculture, Forest Service; U.S. Department of Interior, Bureau of Land Management (USDA and USDI), 1994, Record of decision for amendments to Forest Service and Bureau of Land Management planning documents within the range of the northern spotted owl, [place of publication unknown], 74 p.

Warren, S.D., Hohmann, M.G., Auerswald, K., and Mitasova, H., 2004, An evaluation of methods to determine slopes using digital elevation data: Catena. v. 58, p. 215-233.

Whitacre, H.W., Roper, B.B., and Kershner, J.L., 2007, A comparison of protocols and observer precision for measuring physical stream attributes: Journal of the American Water Resources Association, v. 43, p. 923-937.

Williams, G.P., 1978, Bank-full discharge of rivers: Water Resources Research, v. 14, no. 6, p. 1141–1154.

Woodsmith, R.D., and Buffington, J.M., 1996, Multivariate geomorphic analysis of forest streams: Implications for assessment of land use impact on channel condition: Earth Surface Processes and Landforms, v. 21, p. 377-393.

Wright, C.W., Brock, J.C., Nayegandhi, N., and Kinzel, P.J., 2006, The NASA Experimental Advanced Airborne Research LiDAR: A cross-environment LiDAR: EOS Transactions, American Geophysical Union, v. 87, no. 52, Fall Meeting Supplement, Abstract G53E-04.

Young, M.K., Mace, E.A., Ziegler, E.T., and Sutherland, E.K., 2006, Characterizing and contrasting instream and riparian coarse wood in western Montana basins: Forest Ecology and Management, v. 226, p. 26-40.